Wideband Low Sidelobe Slot Array Antenna with Compact Tapering Feeding Network for E-Band Wireless Communications

Liu, Peiye; Pedersen, Gert Frølund; Zhang, Shuai

Wideband Low Sidelobe Slot Array Antenna with Compact Tapering Feeding Network for E-Band Wireless Communications

Peiye Liu, Gert Frølund Pedersen, *Senior Member IEEE*, Shuai Zhang, *Senior Member IEEE*

Abstract—In this work, a wideband low sidelobe slot array antenna for wireless communication system at E-band is presented. The slots are excited by a parallel feeding network where the Taylor distribution is applied. Two types of wideband unequal power divider with compact structures are designed for various output ratios to fit the limited feeding network space. One is integrated vertically inside a 2×1 elements subarray using a set of pins with asymmetrical offset. The other type is designed inside an E-plane T-junction with unbalance impedance at two output ports. To avoid main lobe tilt and asymmetrical radiation patterns, the feeding network is designed to be biaxially symmetrical, and the feed port is placed in the center of the back. A prototype is fabricated with brass and measured in an anechoic chamber. It achieves a peak gain of 25.8 dBi and a fractional impedance bandwidth of 19.2 % with S_{11} below −10 dB. The measured radiation patterns agree with the simulated patterns very well, and the sidelobe level is lower than −21 dB.

Index Terms—Slot array antenna, low sidelobe, wideband, unequal power divider, Taylor distribution, E-band.

I. INTRODUCTION

IN recent years, the fifth-generation (5G) wireless communication system has attracted a high level of interest and developed rapidly. To cater to the growing demand for fast and reliable network access, such as high definition video and virtual reality, the 5G system is required to have high capacity and low latency [1]. The challenge of increased capacity pushed the attention towards high-frequency bands. In particular, with relatively small atmospheric path loss of around 0.4 dB/km and ultrahigh capacity [2], E-band (71-76GHz and 81-86GHz) gets lots of attention in wireless communication [3] [4]. Conventionally, the directive communication link is realized using reflector antennas, which have been mass-produced in the industry. However, reflector antennas are costly and inconvenient in manufacturing, packaging, delivery, and installation with bulky structures. On the other hand, the thin planar array antenna with its low profile and lightweight is one of the most attractive replacements for the reflector antenna.

However, to truly substitute the conventional reflector antenna, challenges still exist. One is the high antenna gain and efficiency requirement. A commonly printed antenna such as a patch array with a microstrip line feeding network is flexible in design and manufacture. However, it is unacceptable due

Peiye Liu, Gert Frølund Pedersen, and Shuai Zhang are with the Antennas, Propagation and Millimeter-wave Systems section at the Department of Electronic Systems, Aalborg University, Denmark (Corresponding author: Shuai Zhang, email: {liu,gfp,sz}@es.aau.dk).

to high ohmic losses in high-frequency bands in large arrays as reported in [5] [6]. Less severe, but the situation is the same with a substrate integrated waveguide (SIW) as reported in [7]. On the other hand, metal-based waveguides such as hollow and gap waveguides with low losses are more suitable for millimeter-wave applications. Many hollow waveguides or gap waveguides fed slot array antennas at high frequency with high gain and wideband characteristics have been reported in [8]–[10], and most of them are uniformly fed. While due to the array factor characteristic, the first sidelobe level (SLL) of uniformly fed arrays is around −13.2 dB. The application is limited by its high SLL, which increases the intensity of the clutter received in the main lobe. The antenna is preferred to have low sidelobe characteristics to reduce the interferences from unexpected sources. One method to suppress the SLL proposed in [11] is to incline the array for 45° by adding one additional layer on the top, and then it will have low SLL performance at the desired orthogonal axes. However, it doubles the thickness of the radiating layer. In [12], the radiating slots are tilted by only 10° to achieve low SLL. A continuous transverse stub array described in [13] achieves high gain and wide bandwidth, but only the H-plane SLL is suppressed. However, these structures cannot solve the problem as it requires that the SLL in all azimuth angles needs to be suppressed. An aperiodic slot array with uniform excitation is proposed in [14], and its maximum SLL in all azimuth angles is −18 dB. However, its relative bandwidth is only 13.6 % which cannot be migrated to cover E-band. To realize low SLL in all azimuth angles, many researchers turn back to the traditional Taylor distribution in the feeding network [15]. A significant effort is put into series-fed arrays. Due to the high gain requirement, a certain amount of radiating elements is needed, excited by a large feeding network. However, a series-fed network suffers from the long-line effect, which significantly reduces the bandwidth as the element number increases, as reported in [16]. In [17], a double layer parallel-fed slot array antenna is proposed. A Taylor distribution is applied in the feeding network layer while each output excites a cavity-backed 2 by 2 slots subarray. While inside the cavity, four slots are fed with the same amplitude and phase. However, it doubles the element spacing to larger than one wavelength, which leads to an SLL increase at around 30° to 50° tilt. And its SLL at 30° to 50° tilt is even higher than the first SLL. Another method to suppress the SLL increase is introduced in [18], which adds a double-slit layer on the top of the slots. However, it increases the overall thickness and complexity of

the structure. Also, the bandwidth is not wide enough.

This paper presents an 8 × 8 slots array antenna with a compact structure. The Taylor distribution is applied with each radiating slot as a tapering unit. Two types of compact wideband unequal power divider with good amplitude tapering and phase balance are introduced to fit the limited feeding network space. Then the complete antenna is designed to be symmetrical by two axes to avoid main lobe tilt and radiation patterns distortion due to the high sensitivity to the tapering feed. Based on these studies, the proposed antenna shows high efficiency and low SLL characteristics. Moreover, the operating frequency is 71 GHz to 86 GHz, which covers the whole required frequency range in E-band.

The paper is organized as follows. The structure of the proposed antenna and the Taylor distribution in the design are shown in section II. In section III, the antenna subarray with the E-plane feeding network is described. Section IV presents two types of wideband compact unequal power divider to realize the expected amplitude distribution. In section V, the whole corporate feeding network and the complete antenna with 8 × 8 elements are optimized. Section VI shows the measured results of the prototype and analysis. Finally, conclusions are drawn in Section VII.
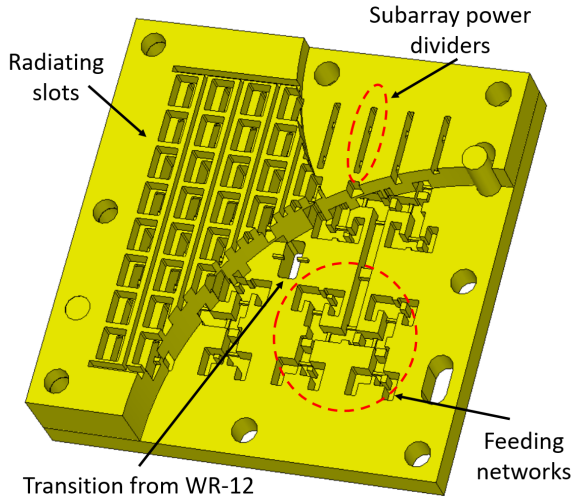
II. ANTENNA GEOMETRY

Fig. 1. The proposed antenna structure.

Fig. 1 shows the structure of the proposed antenna. The total size of the antenna is 32 mm by 32 mm with a height of 7 mm, while the radiating aperture is 28 mm by 28 mm. It consists of three layers. In the top layer, typical slots with cavities are used as the radiating elements. The feeding network is cut into two parts in the middle. The middle layer consists of the subarray power divider shown in the front and half of the feeding network hidden in the back. Moreover, a transition from the standard waveguide WR-12 is also partly hidden in the middle layer's back, which can be seen clearly in section VI. The bottom layer contains the lower part of the feeding network and the feeding port in the center. Screws around the edges

stacked up these layers to minimize the leakage through the gaps between adjacent layers and the corresponding conductor loss.

In the feeding network, a Taylor distribution is applied [15]. Unlike in former studies [17] and [18], subarrays of 2 × 2 slots are used as distribution units, while the four elements inside the subarray are fed with the same amplitude and phase. In this design, amplitude distribution is applied with each radiating slot as an independent unit. The target first SLL is −25 dB with a Taylor $\widetilde{N} = 4$ synthesis. The element spacing (d_{es}) is chosen to be 3 mm, which corresponds 78.5 % of the wavelength in free space at the center frequency. Calculations are done in Matlab while a line array with eight elements is applied. The aperture field distribution is shown in Fig. 2 compared with the conventional 2 × 2 elements subarray unit distribution.
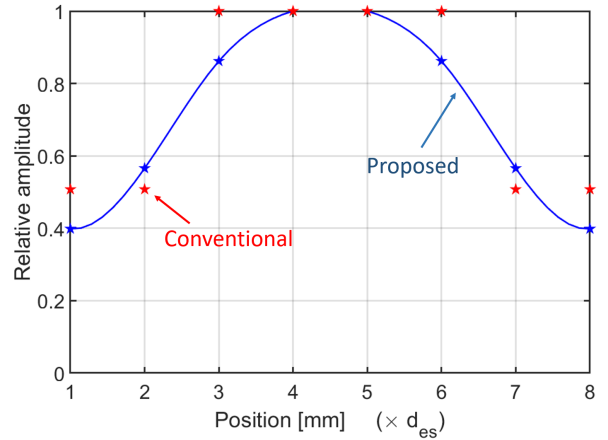

Fig. 2. Aperture field distributions.

Then, the calculated aperture field is applied to a line array. Array factors of the proposed distribution and conventional 2 × 2 elements subarray unit distribution are both depicted in Fig. 3 for comparison [18]. The SLL envelope is smooth in the proposed distribution, and the sidelobes at 30° to 50° tilt are suppressed by around 7 dB.
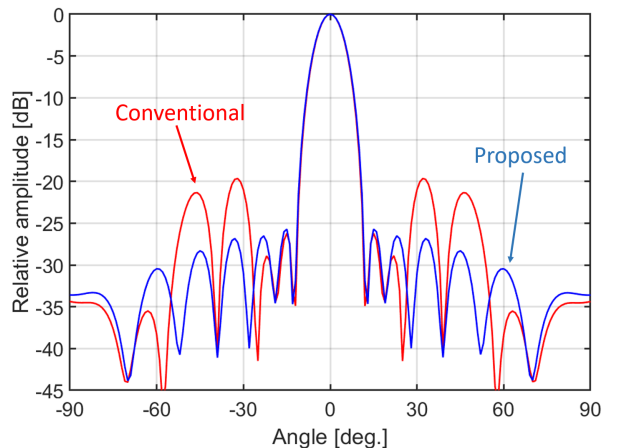

Fig. 3. Array factors.

III. Design of the Subarray

As mentioned above, to apply tapering amplitude distribution in each element, they must be excited independently. In this section, a subarray consist of only two elements is proposed, as shown in Fig. 4. It consists of three layers. The top layer is the radiating layer with two slots arranged in the H-plane and cavities on top to suppress the mutual coupling. The second is the power divider layer, where amplitude tapering in the H-plane is applied, which is discussed in Section IV. The power divider layer is fed by a coupling aperture from the feeding network layer below. The structure minimizes the size of the feeding branch in the bottom layer. It enables T-junction power dividers to be implemented within the limited space, especially in the E-plane where SLL suppression is stricter than in the H-plane. The subarray is optimized using the CST Microwave Studio (CST) with periodic boundaries. All the corners are changed to round with a radius of 0.1 mm. The material used in the simulation is brass (65 %) with electric conductivity of 1.59×10^7 S/M from the CST material library, which is similar to the material going to be used in the fabrication. The surface roughness is set to be 0.0008 mm. Optimized parameters of the subarray are listed in Table I.
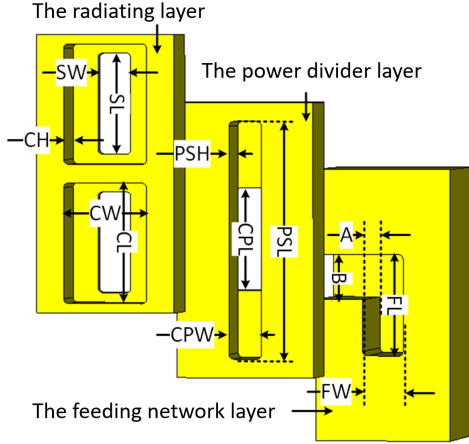

Fig. 4. The Subarray of 2×1 slots.

IV. Design of Compact Unequal power dividers

As plotted above, the antenna elements should follow the amplitude tapering to achieve a radiation pattern with low SLL. Then wideband unequal power dividers with high power-split accuracy are critical to the design. Some H-plane T-junction power dividers have been reported in [19]–[21]. In these structures, the septum is placed with an offset from the feeding branch's centerline to achieve unequal amplitude in two output branches, leading to a large phase difference. Then, one output branch is designed to be longer or narrower than the other to compensate for the phase difference. However, the space required to implement the structure is relatively large. While using a 2×2 slots subarray as a tapering unit, the space limitation is not critical. However, to excite each slot separately in an array with an element spacing of 3 mm, the power divider must fit into a maximum width of around 2 mm

Table I. Optimized parameters of the subarray in Fig. 4.

Width of the radiating slot [SW]	0.7mm
Length of the radiating slot [SL]	2.2mm
Width of the cavity [CW]	1.8mm
Length of the cavity [CL]	2.6mm
Height of the cavity [CH]	1.15mm
Width of the coupling slot [CPW]	0.7mm
Length of the coupling slot [CPL]	2.25mm
Length of the power-split cavity [PSL]	5.2mm
Height of the power-split cavity [PSH]	1.28mm
Width of the feeding line 1 [FW]	0.9mm
Length of the feeding line 1 [FL]	2.25mm
Depth of the feeding line [A]	2.6mm
Width of the feeding line 2 [B]	1.2mm

which corresponds to 47 % of the wavelength at the lowest frequency edge. The septum offset method is no longer available. In this section, two types of wideband unequal power divider with compact structure, good amplitude tapering, and phase balance are proposed. The complete feeding network is designed to be biaxially symmetrical. So only three power-split ratios are required. As shown in Fig. 5, two subarray power dividers with ratios A and B and three feeding network power dividers marked as A, B, and C are designed.
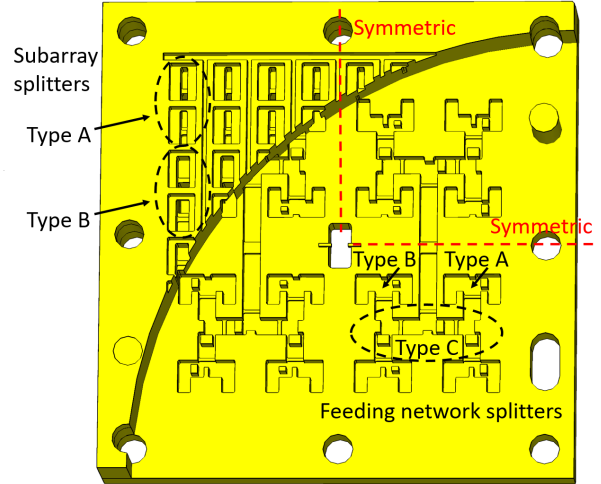

Fig. 5. Top view of the subarray and the feeding network power dividers.

A. Design of Subarray Power Dividers

First of all, an unequal power-split structure in the 2×1 slots subarray is designed. The proposed structure is shown in Fig. 6, one set of pins is put inside the power-split layer. Two pins have the same physical size. The edge of one pin is aligned with the coupling aperture, and the other one has an offset from the edge of the coupling aperture.

The power tapering is achieved by offsetting one pin, which adopts different path characteristics. The power-split ratio is
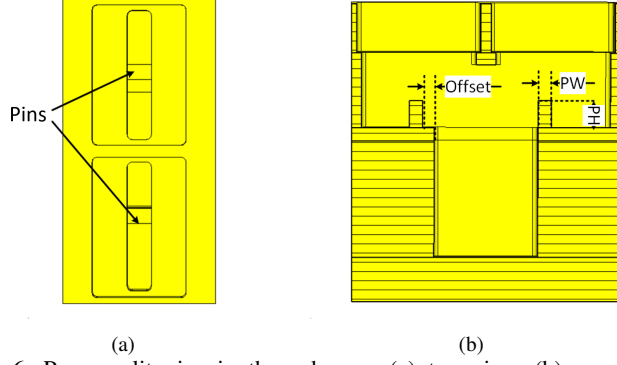
Fig. 6. Power-split pins in the subarray. (a) top view. (b) cross-sectional view.

controlled by the height of the pins (PH). The ratio gets big as the height increases and therefore introduces phase difference between the two output branches. Then the phase difference is balanced by the pin's width (PW). Here in the design, the offset distance is fixed at 0.3 mm, the length of the pin is the same as the coupling aperture width. Then by changing the pin height and width, different power-split ratios are obtained. In subarrays, only two power-split ratios are required. Aperture field distribution calculated in section III is transformed into dB. The ratio for subarrays by the edge of the array (type A) is 3.35 dB, those in the middle (type B) is 1.3 dB.
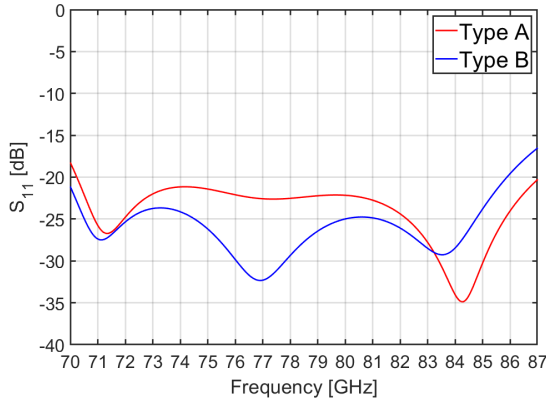
(a)
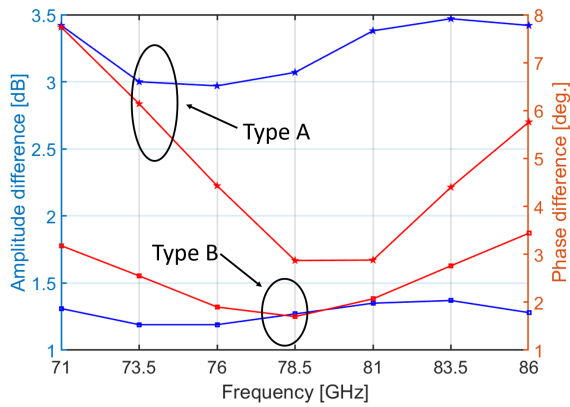
(b)

Fig. 7. Simulation results of subarrays. (a) S-parameters. (b) Amplitude and phase difference between outputs.

Optimizations are done with periodic boundaries too. Although the result is not the same as in a real array (the situation is the same with open boundaries), the variations are acceptable to assess the power-split performance. Optimized PW is 0.3 mm in both subarrays, and PH for the subarray A and B are 0.6 mm and 0.2 mm, respectively. In Fig. 7(a), the S-parameters of the two subarrays shows good matching in the operating frequency band. The amplitude and phase difference is monitored using the 1-D field plot of the E-field monitor function in CST. The results are plotted in Fig. 7(b). The amplitude difference of subarray A is within 3.35 ±0.4 dB, while the phase difference is within 8°. As the power-split ratio is small for subarray type B, the output amplitude fluctuation is relatively small. Its amplitude difference is within 1.3 ±0.11 dB and the phase difference is smaller than 3.5°.

B. Design of Feeding Network Power Dividers

To solve the limited space problem mentioned above, a new compact wideband unequal E-plane T-junction power divider for the feeding network is designed, as shown in Fig. 8.
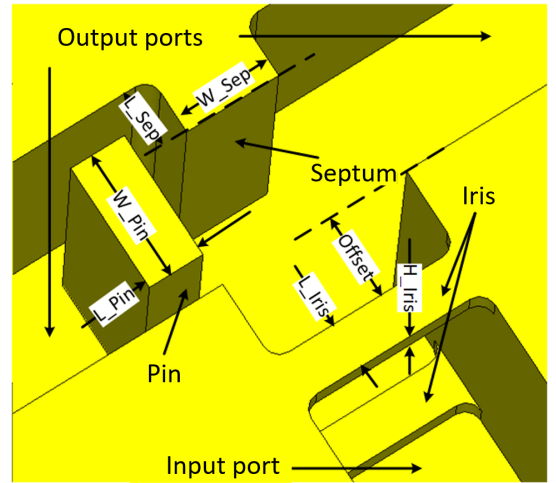

Fig. 8. The 3-D view of the compact unequal E-plane T-junction power divider.

The top metallic plate is hidden in the figure so the T-junction's geometries can be clearly viewed. The E-plane T-junction is symmetric with the centerline of the input port. Two output branches are with the same cross-section and length. The septum lies in the middle of the structure without any offset. Together with the irises, the septum's length and width are optimized for impedance matching. The proposed structure is based on E-plane T-junction. Besides the space limitation, if the septum offset method in [19]–[21] is applied here, the power-split ratio is quite sensitive to frequency. As the jointed T-section is along the narrow edge of the waveguide, it is challenging to achieve wideband performance. In this design, a pin is placed at the center of one branch to introduce different output amplitudes. The power-split ratio between the two output ports can be controlled by turning the pin width and waveguide width ratio. The bigger the width ratio is, the less power is guided into the branch, then the bigger the power-split ratio is. Also, the power-split ratio gets

(a)

(b)

Fig. 10. The 3-D view of (a) H-plane to E-plane T-junction. (b) Transition from the standard waveguide WR-12.
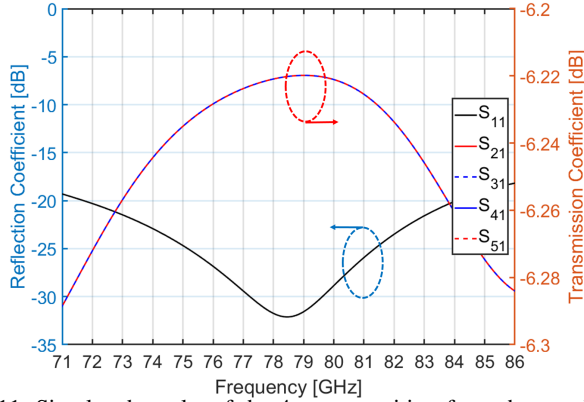
Fig. 11. Simulated results of the 4-way transition from the standard waveguide WR-12.

The transmission loss is smaller than 0.29 dB. In Table IV, the optimized parameters of the 4-way transition from standard waveguide WR-12 are listed.

B. Simulation of the Whole Antenna

After combining these parts, the complete antenna is formed with a biaxial symmetric structure. An extra layer with a thickness of 5 mm is put at the back of the antenna for screws from the mixer. A rectangular slot with the same size as the standard waveguide WR-12 is in the center. 4 mm extension is added at each edge for the positioning pins and screws that stack all the layers up. Gaps between elements along E-plane are added to suppress the mutual coupling. The whole antenna is simulated with open boundary (add space) condition

Table IV. Optimized parameters of the 4-way transition.

Width of the stage (W_ tg)	0.76mm
Height of the stage 1 (H_ tg1)	0.65mm
Length of the stage 1 (L_ tg1)	0.5mm
Height of the stage 2 (H_ tg2)	0.55mm
Width of the probe (W_ P)	0.2mm
Length of the probe (L_ P])	0.84mm
Length of the probe head (L_Pa)	0.2mm
Height of the probe head (H_ P)	0.37mm

in CST, and the simulated amplitude and phase difference of the elements is monitored with the 1-D field plot function and shown in Fig. 12.

(a)

(b)
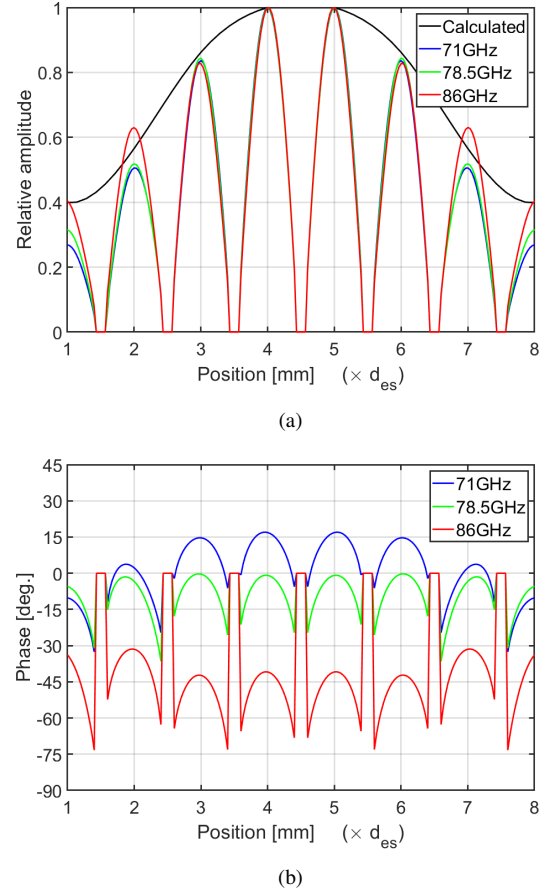
Fig. 12. Normalized (a) amplitude and (b) phase difference at different frequencies.

The elements monitored are those in the center along the H-plane. It can be noticed that both amplitude and phase are pretty symmetrical. The integer numbers in the x-label correspond to the center position of elements. The zero amplitude and phase points in the plots correspond to the cavity walls between elements. In Fig. 12(a), the amplitude of elements in the middle agrees with the calculated relative amplitude quite well. There is a bit of deduction in far elements due to the extended edges, which affects the tapered amplitude of the edge elements. In Fig. 12(b), the phase almost levels between elements at 78.5 GHz. For edge frequencies, the difference between not edge elements is within $15°$.

The radiation patterns are plotted in Fig. 13. The SLL is below -21 dB in all planes and frequencies, no grating lobe appears at around $30°$ to $50°$ tilt. There are variations in SLL as the amplitude tapering distribution and phase are not stable with frequencies. The best performance with SLL smaller than -25 dB is at 78.5 GHz which agrees with amplitude and phase balance monitored. The highest SLL is observed in H-plane at 86 GHz.
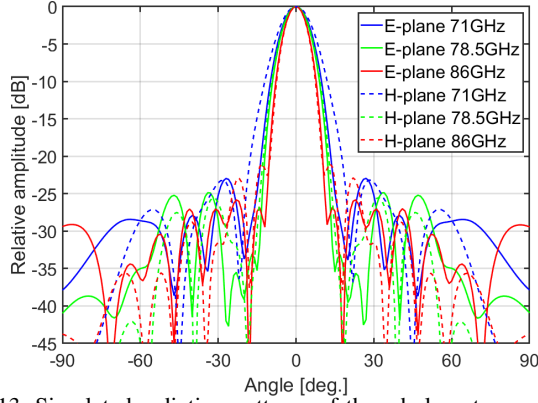
Fig. 13. Simulated radiation patterns of the whole antenna.
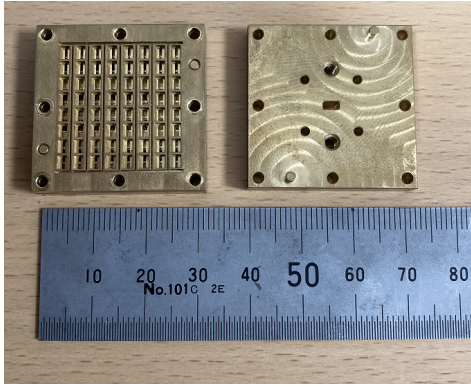
(a)
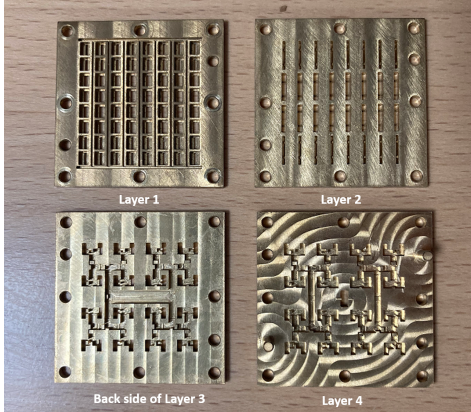
(b)

Fig. 14. Photographs of the fabricated antenna: (a) the assembled antenna and the adapter; (b) each of the layers.

VI. Experimental Results

A prototype is fabricated in the workshop and measured in the anechoic chamber at the Antennas, Propagation and Millimeter-wave Systems laboratory at Aalborg University. Fig. 14 shows the fabricated antenna. The adapter shown in Fig. 14(a) connects the prototype with the mixer. As seen in Fig. 14(b), layer 1 is the radiating layer, and layer 4 is half of the feeding network layer. The middle layer mentioned in section II is separated into two. It is due to the fabrication limitation of our facilities. While without double side alignment technology, positioning accuracy cannot be ensured. Part of the H-plane to E-plane power divider and the transition from

the standard waveguide WR-12 is shown in the back of layer 3. The prototype is fabricated with brass using computerized numerical control (CNC) machine (DMG ecoMill 50) which has a position accuracy of ±0.006 mm. An external spindle (Nakanishi HES510) is used. It goes up to 50 000 RPM and has a spindle runout within 0.001 mm. The end mills have a tool accuracy within 0.002 mm. The surface roughness is controlled below 0.0008 mm in the fabrication.
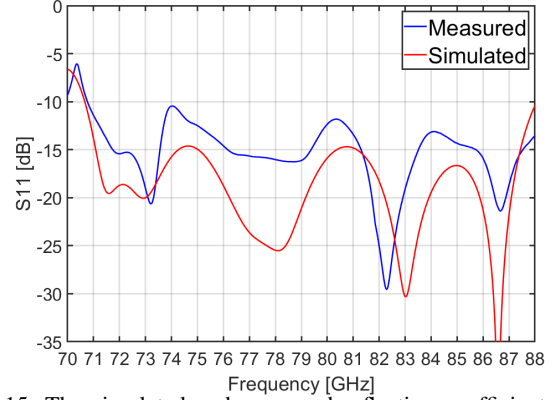
Fig. 15. The simulated and measured reflection coefficients of the prototype.

Fig. 15 shows the measured and simulated reflection coefficients. In the simulation, A result smaller than −14 dB can be achieved in the frequency band from 71 to 87.4 GHz. The measured reflection coefficient distorts to some extent but can still maintain below −10 dB over the targeted band from 71 to 86 GHz.

The distortion is mainly due to fabrication tolerance and misalignment in assembling, which may change the impedance characteristics of the feeding network. In our design, the distribution network is designed by hollow waveguides with an E-plane split. By using this method, the surface current inside the hollow waveguide is continuous as possible, and good electric contact is not so strictly required as the waveguides are separated in the middle where the current flow is minimal [23]. Therefore, the corresponding conductor loss can be minimized. Compared with the air gap between the two metal layers containing the feeding network, other gaps are less sensitive. As they are vertical waveguide cuts in an orthogonal plane, and small air gaps will not affect the vertical propagation characteristic much. To minimize power leakage, these gaps are preferred as small as possible. First, good fabrication accuracy is applied. Then, as the antenna is only with eight by eight elements, its size is correspondingly small. So the flatness of the layers can be ensured to some extent. Moreover, eight screws around the edges are used to stack these layers up for good metal contact.

An analysis of the air gap effect is carried out and illustrated in Fig. 16. Air gaps of 0, 10, 25, and 50 μm between all layers are compared. Gain (IEEE) from CST is checked as it does not consider the reflection coefficient but only ohmic losses. The only variable is the air gap size. As the air gap goes up to 10 μm, the gain does not decrease much. However, from 25 to 50 μm gaps, the gain drops significantly. From the

simulated results, a good metal contact between the layers can be confirmed.
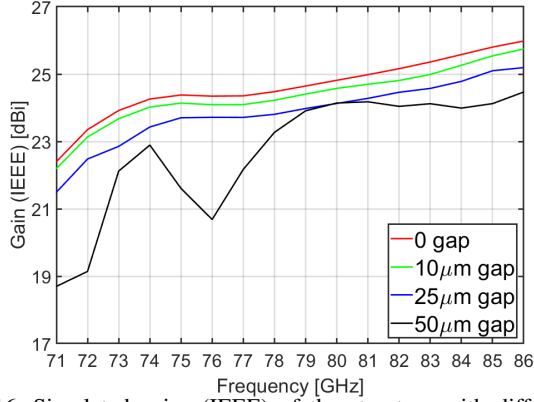
Fig. 16. Simulated gains (IEEE) of the structure with different air gap sizes.

Fig. 17 shows the measured radiation patterns of the middle and edge frequencies at different planes. The ETSI Class II mask [24] is also depicted in the figures. It can be seen that besides the measured patterns at 71 GHz, which are slightly distorted, the others are all symmetrical and satisfy the class II sidelobe envelope requirement and agree with the simulated quite well. The distortion at 71 GHz is mainly because the prototype is assembled with metal screws while the screw's head appeared on the antenna's front side. As the height of the screw head is close to the half-wavelength at 71 GHz, the patterns are distorted more severely than other frequencies. Also, the fabrication and assemble inaccuracy may cause distortions to some extent as the impedance characteristics are changed. The element spacing of the proposed antenna is 3 mm, which corresponds to 86% of the wavelength at 86 GHz in free space. It is pretty close to the no grating lobe condition of 89% [25]. Since the amplitude tapering distribution and phase unbalance could raise the restrictions to some extent, the SLL in the E-plane of 86 GHz at ±90° is higher than the desired. It can be noticed that the simulated backlobes also hit the mask. However, it is less critical than the SLL requirement. Since in the application, the antenna is installed inside an outdoor unit (ODU), while a large metal cavity is put at the backside of the antenna, the backlobes will be effectively suppressed. One more thing that should be mentioned is that the measured backlobes in all the patterns are not trustable. An absorber is placed between the antenna and the mixer in the measurement. Because the reflection from the mixer is severe at such high frequency and could cause ripples in the main lobe, it leads to an inaccurate gain. Despite the distortion, SLL in all patterns remains below −21 dB, which is reasonably good. The cross-polarization level stays above 27 dB for all frequencies and cuts. It is higher than that of the general rectangular slot array antenna due to the unidentical amplitude excitation, and phase unbalances between adjacent units. As a result, the cross-polarized component coupled from adjacent units and the cross-polarized component generated by the local unit cannot fully be compensated.

The simulated and measured realized gains are shown in

(a) E-plane 71GHz   (b) H-plane 71GHz

(c) E-plane 78.5GHz   (d) H-plane 78.5GHz

(e) E-plane 86GHz   (f) H-plane 86GHz
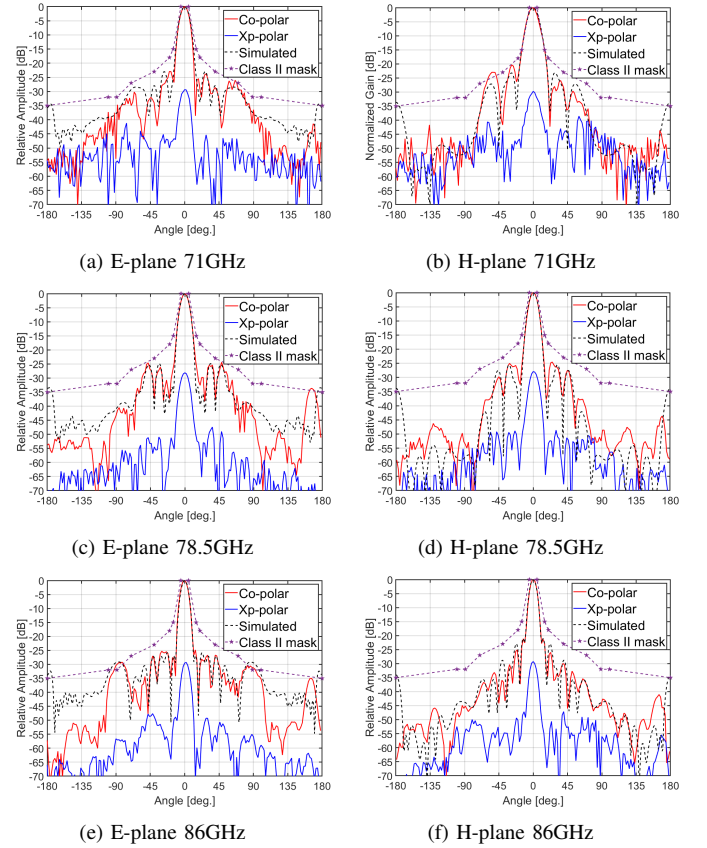
Fig. 17. Measured Co-polar and cross-polar radiation patterns compared with simulated patterns at (a) E-plane 71GHz, (b) H-plane 71GHz, (c) E-plane 78.5GHz, (d) H-plane 78.5GHz, (e) E-plane 86GHz, (f) H-plane 86GHz.

Fig. 18. The measured gain is higher than 22.1 dBi in the bandwidth of 71 to 86 GHz with antenna efficiency of around 70%. There are also some gain variations in the measurement. It is mainly due to the measurement tolerance. Furthermore, the amplitude tapering distribution and phase are not entirely stable with frequencies, which may also cause gain variations.
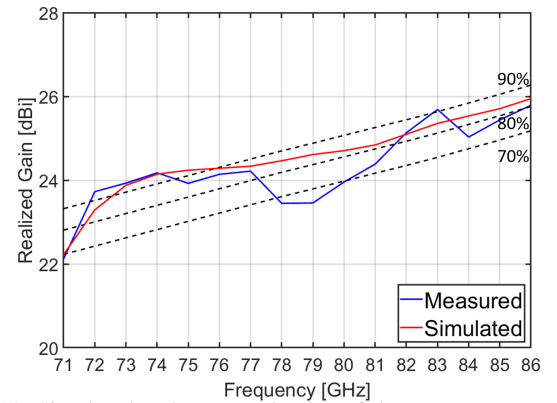
Fig. 18. Simulated and measured gains of the prototype.

Table V shows a comparison between the proposed antenna and various reported planar array antennas with low SLL characteristics. Low SLL in all azimuth planes is achieved in this work. The proposed antenna has a wide impedance bandwidth with a correspondingly low maximum SLL compared

Table V. Compared results between the proposed and reported low SLL array antennas.

Works	Aperture size ($\lambda \times \lambda$)	No of elements	Frequency (GHz)	Impedance bandwidth (-10 dB), (%)	Efficiency (%)	3-dB beamwidth (in the suppressed axes), (°)	Maximum SLL (in all azimuth angles), (dB)
Ref. [11]	15.5×15.6	16×16	57 - 67	17.6	60	unknown	-13.2
Ref. [13]	43.2×25.1	32	71 - 86	19.2	38	2.85 - 3.6	-13.2
Ref. [14]	11.1×8.5	160	27.5 - 31.5	13.6	70	around 10	-18
Ref. [16]	7.27×7.27	76	8.9	0.34	30	8.9 - 9	-28.8
Ref. [17]	12.18×12.18	16×16	14.2 - 16.2	13.8	70	5.1-5.3	around -23
Ref. [18]	17.75×17.75	16×16	71 - 76	6.8	70	around 6.7	-20
This work	8.4×8.4	8×8	71 - 86	19.2	70	8.6 - 12.9	-21

to others. Besides, in [17], the first SLL smaller than 24.1 dB is achieved. However, significant sidelobes (around -23 dB) at $30°$ to $50°$ tilt are observed, which will severely exceed the ETSI class II mask. In the present work, no apparent SLL increase at $30°$ to $50°$ tilt is observed, and satisfaction of the ETSI class II mask can be confirmed over most of the frequencies.

VII. CONCLUSION

In this paper, a wideband 8×8 slots array antenna is reported. Two types of wideband unequal power divider are designed. By applying these power dividers in the feeding network, each radiating slot is excited independently with the Taylor distribution calculated. A prototype is fabricated and measured. At the design frequency from 71 GHz to 86 GHz, the measured radiation patterns agree with the simulated ones well, and the SLL in all planes is below -21 dB. A realized gain of over 22.1 dBi with antenna efficiency of around 70 % is achieved within the fractional impedance bandwidth of 19.2 %. Theoretically, the gain of a large array with 64×64 elements can meet the requirement of 38 dBi in the point-to-point communication [24]. Morever, satisfaction with the ETSI class II mask can be confirmed. The proposed structure shows that the slot array antenna has the potential to substitute the conventional reflector antenna in a wireless communication system.

REFERENCES

[1] M. Jaber, M. A. Imran, R. Tafazolli, and A. Tukmanov, "5G backhaul challenges and emerging research directions: A survey," *IEEE Access*, vol. 4, pp. 1743–1766, 2016.

[2] D. Lockie and D. Peck, "High-data-rate millimeter-wave radios," *IEEE Microw. Mag.*, vol. 10, no. 5, pp. 75–83, 2009.

[3] F. Boes, J. Antes, T. Messinger, D. Meier, R. Henneberger, A. Tessmann, and I. Kallfass, "Multi-gigabit E-band wireless data transmission," in *2015 IEEE MTT-S International Microwave Symposium*, pp. 1–4, 2015.

[4] X. Li, J. Xiao, and J. Yu, "Long-distance wireless mm-wave signal delivery at W-Band," *J. Light. Technol.*, vol. 34, no. 2, pp. 661–668, 2016.

[5] W. Yang, K. Ma, K. S. Yeo, and W. M. Lim, "A compact high-performance patch antenna array for 60 GHz applications," *IEEE Antenna Wireless Propag. Lett.*, vol. 15, pp. 313–316, 2016.

[6] S. Yoo, Y. Milyakh, H. Kim, C. Hong, and H. Choo, "Patch array antenna using a dual coupled feeding structure for 79 GHz automotive radar applications," *IEEE Antenna Wireless Propag. Lett.*, vol. 19, no. 4, pp. 676–679, 2020.

[7] Y. Yu, W. Hong, Z. H. Jiang, and H. Zhang, "E-band low-profile, wideband 45° linearly polarized slot-loaded patch and its array for millimeter-wave communications," *IEEE Trans. Antennas Propag.*, vol. 66, no. 8, pp. 4364–4369, 2018.

[8] Y. Miura, J. Hirokawa, M. Ando, Y. Shibuya, and G. Yoshida, "Double-layer full-corporate-feed hollow-waveguide slot array antenna in the 60 GHz band," *IEEE Trans. Antennas Propag.*, vol. 59, no. 8, pp. 2844–2851, 2011.

[9] A. Vosoogh and P.-S. Kildal, "Corporate-fed planar 60 GHz slot array made of three unconnected metal layers using AMC pin surface for the gap waveguide," *IEEE Antenna Wireless Propag. Lett.*, vol. 15, pp. 1935–1938, 2016.

[10] P. Liu, J. Liu, W. Hu, and X. Chen, "Hollow waveguide 32×32-slot array antenna covering 71–86 GHz band by the technology of a polyetherimide fabrication," *IEEE Antenna Wireless Propag. Lett.*, vol. 17, no. 9, pp. 1635–1638, 2018.

[11] T. Tomura, Y. Miura, M. Zhang, J. Hirokawa, and M. Ando, "A 45° linearly polarized hollow-waveguide corporate-feed slot array antenna in the 60 GHz band," *IEEE Trans. Antennas Propag.*, vol. 60, no. 8, pp. 3640–3646, 2012.

[12] A. Vosoogh, P.-S. Kildal, and V. Vassilev, "Wideband and high-gain corporate-fed gap waveguide slot array antenna with ETSI Class II radiation pattern in *V*-Band," *IEEE Trans. Antennas Propag.*, vol. 65, no. 4, pp. 1823–1831, 2017.

[13] T. Potelon, M. Ettorre, L. Le Coq, T. Bateman, J. Francey, D. Lelaidier, E. Seguenot, F. Devillers, and R. Sauleau, "A low-profile broadband 32-slot continuous transverse stub array for backhaul applications in *E*-Band," *IEEE Trans. Antennas Propag.*, vol. 65, no. 12, pp. 6307–6316, 2017.

[14] L. Shi, C. Bencivenni, R. Maaskant, J. Wettergren, J. Pragt, and M. Ivashina, "High-efficiency and wideband aperiodic array of uniformly excited slotted waveguide antennas designed through compressive sensing," *IEEE Trans. Antennas Propag.*, vol. 67, no. 5, pp. 2992–2999, 2019.

[15] C. A. Balanisn, "Antenna theory: Analysis and design," in *3rd ed. Hoboken,NJ, USA: Wiley*, p. 406–408, 2005.

[16] P. Kumar, A. Kedar, and A. K. Singh, "Design and development of low-cost low sidelobe level slotted waveguide antenna array in X-Band," *IEEE Trans. Antennas Propag.*, vol. 63, no. 11, pp. 4723–4731, 2015.

[17] G.-L. Huang, S.-G. Zhou, T.-H. Chio, H.-T. Hui, and T.-S. Yeo, "A low profile and low sidelobe wideband slot antenna array feb by an amplitude-tapering waveguide feed network," *IEEE Trans. Antennas Propag.*, vol. 63, no. 1, pp. 419–423, 2015.

[18] H. Arakawa, H. Irie, T. Tomura, and J. Hirokawa, "Suppression of e-plane sidelobes using a double slit layer in a corporate-feed waveguide slot array antenna consisting of 2×2 -element radiating units," *IEEE Trans. Antennas Propag.*, vol. 67, no. 6, pp. 3743–3751, 2019.

[19] G.-L. Huang, S.-G. Zhou, T.-H. Chio, and T.-S. Yeo, "Design of a symmetric rectangular waveguide T-junction with in-phase and unequal power split characteristics," in *2013 IEEE Antennas and Propagation Society International Symposium (APSURSI)*, pp. 2119–2120, 2013.

[20] S. Yang and A. Fathy, "Synthesis of a compound T-junction for a two-way splitter with arbitrary power ratio," in *IEEE MTT-S International Microwave Symposium Digest, 2005.*, pp. 985–988, 2005.

[21] S. Christopher, V. Abid Hussain, M. Easwaran, and V. Dabade, "Design aspects of compact high power multiport unequal power dividers," in *Proceedings of International Symposium on Phased Array Systems and Technology*, pp. 63–67, 1996.

[22] J. Liu, A. Vosoogh, A. U. Zaman, and J. Yang, "Design and fabrication of a high-gain 60-GHz cavity-backed slot antenna array fed by inverted microstrip gap waveguide," *IEEE Trans. Antennas Propag.*, vol. 65, no. 4, pp. 2117–2122, 2017.

[23] Z. Shi-Gang, H. Guan-Long, P. Zhao-hang, and L.-J. Ying, "A wideband

full-corporate-feed waveguide slot planar array," *IEEE Trans. Antennas Propag.*, vol. 64, no. 5, pp. 1974–1978, 2016.

[24] "Fixed radio systems characteristics requirements, standard etsi en 302 217-4-2 v1.5.1 (2010-01), european telecommunications standards, 2010. [online]. available: http://www.etsi.org/index.php,"

[25] P.-S. Kildal, *Foundations of Antenna Engineering: A Unified Approach for Line-of-Sight and Multipath*. Artech, 2015.

Shuai Zhang (SM'18) received the B.E. degree from the University of Electronic Science and Technology of China, Chengdu, China, in 2007 and the Ph.D. degree in electromagnetic engineering from the Royal Institute of Technology (KTH), Stockholm, Sweden, in 2013. After his Ph.D. studies, he was a Research Fellow at KTH. In April 2014, he joined Aalborg University, Denmark, where he currently works as Associate Professor and the leader of antennas group. In 2010 and 2011, he was a Visiting Researcher at Lund University, Sweden and at Sony Mobile Communications AB, Sweden, respectively. He was also an external antenna specialist at Bang & Olufsen, Denmark from 2016-2017. He has co-authored over 80 articles in well-reputed international journals and over 16 (US or WO) patents. His current research interests include: mmwave antennas for cellular communications, biological effects, CubeSat antennas, Massive MIMO antennas, wireless sensors, and RFID antennas.

Peiye Liu was born in Harbin, China, in 1985. He received the M.S. degree in wireless and photonics engineering from Chalmers University of Technology, Gothenburg, Sweden, in 2016. After M.S. studies, he joined Guangdong Shenglu telecommunication technology, co., Ltd. Currently, he is a research assistant at the Department of Electronic Systems at Aalborg University. His research interests include planner array antennas, mm-wave mobile antenna design, and interactions between the user and mobile antennas.

Gert Frølund Pedersen was born in 1965. He received the B.Sc. and E.E. (Hons.) degrees in electrical engineering from the College of Technology in Dublin, Dublin Institute of Technology, Dublin, Ireland, in 1991, and the M.Sc.E.E. and Ph.D. degrees from Aalborg University, Aalborg, Denmark, in 1993 and 2003, respectively. Since 1993, he has been with Aalborg University, where he is a Full Professor heading the Antenna, Propagation, and Networking LAB with 36 researchers. He is also the Head of the Doctoral School on wireless communication with some 100 Ph.D. students enrolled. His research interests include radio communication for mobile terminals, especially small antennas, diversity systems, propagation, and biological effects. He has published more than 175 peer-reviewed papers and holds 28 patents. He has also worked as a Consultant for developments of more than 100 antennas for mobile terminals, including the first internal antenna for mobile phones in 1994 with the lowest SAR, the first internal triple-band antenna in 1998 with low SAR and high TRP and TIS, and lately various multiantenna systems rated as the most efficient on the market. He has worked most of the time with joint university and industry projects and has received more than 12 M\$ in direct research funding. He is currently the Project Leader of the SAFE project with a total budget of 8 M\$ investigating tunable front end including tunable antennas for the future multi-band mobile phones. He has been one of the pioneers in establishing over-the-air measurement systems. The measurement technique is now well established for mobile terminals with single antennas. He was chairing the various COST groups (swg2.2 of COST 259, 273, 2100, and now ICT1004) with liaison to 3GPP for an over-the-air test MIMO terminals. He is currently involved in MIMO OTA measurement.